toxins

MDPI

Article

Botulinum Toxin Complex Serotype B-Okra Exerts Systemic Toxicity via the Oral Route by Disrupting the Intestinal Epithelial Barrier

Chiyono Morimoto [1,†], Sho Amatsu [1,2,*,†], Takuhiro Matsumura [1], Masahiko Zuka [2] and Yukako Fujinaga [1,*]

[1] Department of Bacteriology, Graduate School of Medical Sciences, Kanazawa University, Kanazawa 920-8640, Japan; t-matsu@med.kanazawa-u.ac.jp (T.M.)
[2] Department of Forensic Medicine and Pathology, Graduate School of Medical Sciences, Kanazawa University, Kanazawa 920-8640, Japan
* Correspondence: amatsu@med.kanazawa-u.ac.jp (S.A.); yukafuji@med.kanazawa-u.ac.jp (Y.F.)
† These authors contributed equally to this work.

Abstract

Botulinum toxin (BoNT) causes flaccid paralysis by blocking the release of neurotransmitters. BoNTs associate with neurotoxin-associated proteins to form medium and large progenitor toxin complexes. The large progenitor toxin complex serotype A-62A (L-PTC/A-62A) specifically targets intestinal M cells for invasion, whereas large progenitor toxin complex serotype B-Okra (L-PTC/B-Okra) is mainly taken up by enterocytes and exhibits higher toxicity via the oral route. Hemagglutinin (HA) is a neurotoxin-associated protein that promotes BoNT absorption from the intestine and has carbohydrate-binding and barrier-disrupting activities. In this study, we established an in vitro reconstitution and purification system for recombinant L-PTC/B-Okra and created a recombinant L-PTC/B-Okra mutant rL-PTC/B-KA with carbohydrate-binding activity but not barrier-disrupting activity. rL-PTC/B-KA showed significantly reduced oral toxicity. Our results demonstrate that the B-Okra toxin disrupts the epithelial barrier of enterocytes and exerts oral toxicity.

Keywords: *Clostridium botulinum*; botulinum toxin; botulinum toxin complex; in vitro reconstitution; hemagglutinin; E-cadherin; epithelial barrier

Key Contribution: Botulinum toxin complex serotype B-Okra disrupts the epithelial barrier of enterocytes, leading to high oral toxicity.

check for updates

Received: 8 July 2025
Revised: 1 September 2025
Accepted: 2 September 2025
Published: 4 September 2025

Citation: Morimoto, C.; Amatsu, S.; Matsumura, T.; Zuka, M.; Fujinaga, Y. Botulinum Toxin Complex Serotype B-Okra Exerts Systemic Toxicity via the Oral Route by Disrupting the Intestinal Epithelial Barrier. *Toxins* **2025**, *17*, 443. https://doi.org/10.3390/toxins17090443

Copyright: © 2025 by the authors. Licensee MDPI, Basel, Switzerland. This article is an open access article distributed under the terms and conditions of the Creative Commons Attribution (CC BY) license (https://creativecommons.org/licenses/by/4.0/).

1. Introduction

Botulinum toxin (BoNT) is the most potent naturally occurring toxin and is responsible for causing botulism, a life-threatening condition characterized by flaccid paralysis. BoNT blocks neurotransmitter release by cleaving soluble *N*-ethylmaleimide-sensitive-factor attachment protein receptor (SNARE) proteins at the presynaptic terminals of neurons [1]. BoNTs are produced by *Clostridium botulinum* and related species as progenitor toxin complexes (PTCs) with neurotoxin-associated proteins (NAPs) [2]. Neurotoxin-associated proteins comprise a non-toxic non-hemagglutinin (NTNHA) and three hemagglutinins (HAs): HA1, HA2, and HA3 (also known as HA33, HA17, and HA70, respectively). NTNHA associates with BoNT to form a medium progenitor toxin complex (M-PTC) and protects the toxin from digestion and destabilization in gastrointestinal juice [2,3]. The HA complex is assembled from six HA1, three HA2, and three HA3 [4–7], and associates with M-PTC to form

a large progenitor toxin complex (L-PTC), which exhibits approximately 700-fold higher oral toxicity than M-PTC [2,8]. HA facilitates the intestinal absorption of BoNTs through at least two activities: carbohydrate-binding [5,9–14] and barrier-disruption [13–19]. L-PTC binds to the luminal surface of the intestinal epithelial cells via HA's carbohydrate-binding activity [9,20–25]. After transcytosis from the apical to the basolateral surface, HA binds to E-cadherin and inhibits cell–cell adhesion; HA disrupts the epithelial barrier, resulting in the paracellular transport of BoNT across the intestine [15,16,18]. In HA-negative strains, OrfX genes are associated with the BoNT gene instead of HA genes [26]. It has recently been reported that OrfX2 can assemble with M-PTC and boost the oral toxicity [27], although the mechanism remains largely unknown.

BoNTs have been classified into seven serotypes (A–G), of which serotypes A, B, E, and F cause human botulism [28]. L-PTCs are classified as "hyper-oral-toxic (HOT)" or "non-HOT" based on their relative oral toxicity levels [2,8,25]. These classes can be categorized based on the carbohydrate-binding activity of HA [25]. L-PTC serotype A-62A (L-PTC/A-62A), a non-hyper-oral-toxic toxin, targets intestinal microfold (M) cells for entry [23]. Intestinal M cells are specialized epithelial cells with the ability to transport macromolecules and microorganisms from the gut lumen to the underlying lymphoid tissue to induce antigen-specific immune response and are located in the follicle-associated epithelium (FAE) of Peyer's patches [29]. L-PTC/A-62A exerts oral toxicity by disrupting the epithelial barrier around M cells [18,23]. In contrast, L-PTC serotype B-Okra (L-PTC/B-Okra), which exhibits 20–80-fold greater oral toxicity and is classified as HOT-type, is taken up by enterocytes (also known as intestinal absorptive cells) [25].

Enterocytes are the most abundant epithelial cell lineage in the small and large intestine, and especially constitute more than 80% of all epithelial cells in the small intestine [30]. A single layer of enterocytes lining the intestinal epithelium serves as the physical and functional barrier between the luminal contents of the gut and the host [31]. The HA of L-PTC/B-Okra increases the intestinal permeability of fluorescein isothiocyanate (FITC)-dextran and PTCs [15], although the effect of the barrier-disrupting activity of L-PTC/B-Okra on oral toxicity remains unclear. In this study, we established an in vitro reconstitution and purification system for recombinant L-PTC/B-Okra and created a recombinant L-PTC/B-Okra mutant with carbohydrate-binding activity, but not barrier-disrupting activity (rL-PTC/B-KA). Our results demonstrate that the barrier-disrupting activity of the HOT-type toxin L-PTC/B-Okra is critically involved in its toxicity via the oral route.

2. Results

2.1. In Vitro Reconstitution and Purification of Recombinant L-PTC (rL-PTC)

To elucidate the impact of HA differences between L-PTC/B and L-PTC/A on systemic toxicity via the oral route, we created wild-type rL-PTC/B (rL-PTC/B-WT) and a chimeric L-PTC/B comprising HA/A instead of HA/B (rL-PTC/BA-WT) (Figures 1 and 2A–C) [25]. HA3 Lys607 is crucial for the binding of HA to E-cadherin, and its alanine substitution (K607A, KA) impairs E-cadherin binding and barrier-disrupting activities [17]. We also generated rL-PTCs containing HA3-K607A (rL-PTC/B-KA and rL-PTC/BA-KA) (Figure 2B,C). These rL-PTCs contained similar amounts of BoNT/B, NTNHA/B, and HAs (Figure 2B,C).

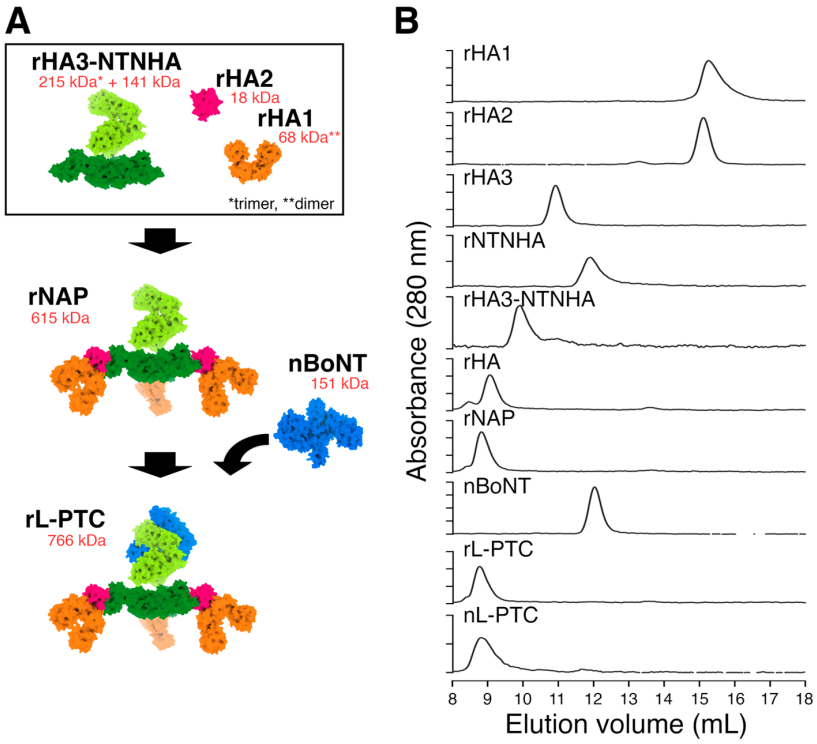


Figure 1. In vitro reconstitution of recombinant large progenitor toxin complex derived from *C. botulinum* serotype B-Okra (rL-PTC/B). (**A**) Schematic model of in vitro reconstitution of rL-PTC, a 766 kDa complex composed of nBoNT, rNTNHA, rHA3, rHA2, and rHA1 in a stoichiometry 1:1:3:3:6. (**B**) Size exclusion chromatography analysis. Recombinant proteins (rL-PTC/B-WT, rNAP/B, rNTNHA/B, and rHAs/B) and native proteins (nL-PTC/B and nBoNT) were subjected to size exclusion chromatography on a Superdex 200 Increase 10/300 GL column. Protein elution profiles were monitored at 280 nm. BoNT, botulinum neurotoxin; NTNHA, non-toxic non-hemagglutinin; HA, hemagglutinin; NAP, neurotoxin-associated protein; rL-PTC, recombinant L-PTC; nL-PTC, native L-PTC; nBoNT, native BoNT. Asterisks indicate the molecular weights of rHA3 as a trimer (*) and rHA1 as a dimer (**).

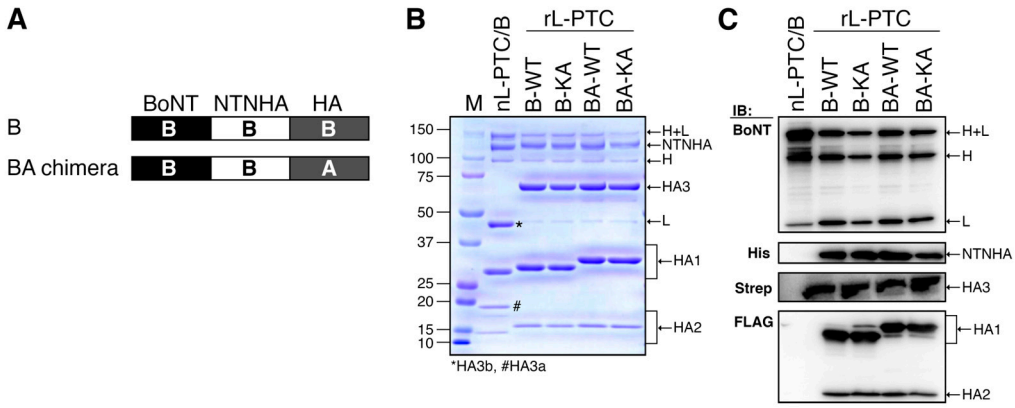


Figure 2. The molecular compositions of the purified rL-PTCs. (**A**) Schematic diagram of rL-PTC serotype B-Okra (rL-PTC/B-WT) and chimeric rL-PTC (rL-PTC/BA-WT) comprising BoNT/B, NTNHA/B, and HA derived from A-62A (HA/A). The purified nL-PTC/B, rL-PTCs/B, and rL-PTCs/BA were analyzed by SDS-PAGE with Coomassie brilliant blue staining (**B**) and Western blotting (**C**). WT: wild type, KA: HA3-K607A mutant. The membranes were probed with anti-BoNT/B antiserum, anti-His tag, anti-Strep tag II, and anti-FLAG tag antibodies, followed by the corresponding horseradish peroxidase-conjugated secondary antibodies. Asterisk (*) and sharp sign (#) indicate C-terminal (HA3b) and N-terminal (HA3a) domains of HA3, respectively. H + L, intact BoNT (heavy chain and light chain); H, heavy chain of BoNT; L, light chain of BoNT; M, marker.

2.2. Carbohydrate-Binding Activity

L-PTC binds to the intestinal epithelium through the carbohydrate-binding activity of HA [9,20–25]. We assessed the carbohydrate-binding activity of rL-PTCs by ELISA using porcine gastric mucin (PGM) and bovine submaxillary mucin (BSM), which mediate galactose- and sialic acid-dependent binding, respectively [17]. rL-PTC/B-WT and rL-PTC/B-KA bound to PGM and BSM in a similar manner of nL-PTC/B (Figure 3). HA/A has more extended carbohydrate-binding pockets than HA/B, and both native L-PTC/A and rHA/A bind mucins with higher affinity than native L-PTC/B and rHA/B [25]. Consistent with this, the chimera toxins rL-PTC/BA-WT and rL-PTC/BA-KA, in which HA/B is replaced with HA/A, bind mucins in a similar manner of native L-PTC/A and rHA/A (Figure 3). These data show that swapping HA in the rL-PTCs alters the carbohydrate-binding spectrum, and that the HA3 K607A mutation does not impair the carbohydrate-binding activities.

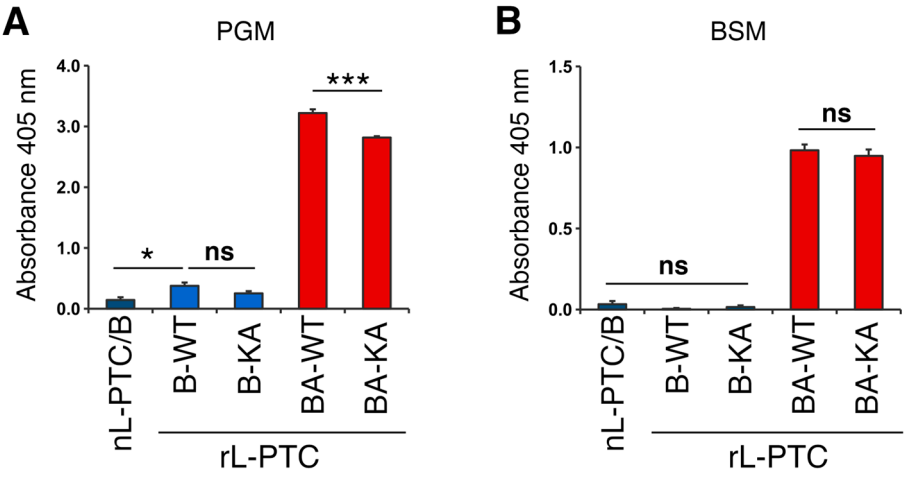


Figure 3. Carbohydrate-binding activities of rL-PTCs. HA-mediated binding of L-PTCs to porcine gastric mucin (PGM, **A**) and bovine submaxillary mucin (BSM, **B**). 10 nM L-PTCs were added to PGM- or BSM-coated ELISA plates, and then the plates were probed with anti-BoNT/B anti-serum. Data are representative of at least four independent experiments. Values are mean ± S.E. of triplicate wells. The data were analyzed by one-way ANOVA with Tukey's HSD post hoc test (* $p < 0.05$, *** $p < 0.001$, ns: not significant).

2.3. Epithelial Barrier-Disrupting Activity

HA/A and HA/B inhibit cell–cell adhesion in epithelial cells by binding to E-cadherin, resulting in epithelial barrier disruption [13–19]. HA2 and HA3^{mini} (aa 380-626) are responsible for the binding of HA to E-cadherin. Notably, the recombinant HA/B harboring the HA3-K607A mutant (rHA/B-KA) is deficient in barrier-disrupting activity [17–19]. Consistent with this, rL-PTC/B-WT and rL-PTC/BA-WT disrupted the epithelial barrier of Caco-2 cell monolayers and exhibited barrier-disrupting activity comparable to that of native L-PTC/B and rHA/A, respectively (Figure 4). These data demonstrate that the wild-type recombinant L-PTCs are fully functional in disrupting the epithelial barrier. In contrast, rL-PTC/B-KA and rL-PTC/BA-KA had no effect on the epithelial barrier function (Figure 4), indicating that the HA3 K607A mutation impairs the barrier-disrupting activities of L-PTCs.

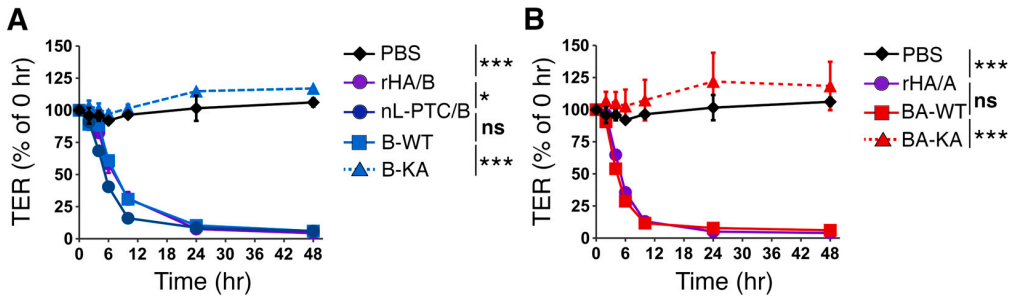


Figure 4. Barrier-disrupting activities of rL-PTCs. 10 nM L-PTCs (nL-PTC/B; rL-PTC/B-WT, B-WT; rL-PTC/B-KA, B-KA; rL-PTC/BA-WT, BA-WT; rL-PTC/BA-KA, BA-KA) and rHAs (rHA/B, rHA/A) ((**A**): serotype B-Okra, (**B**): serotype A-62A and rL-PTCs/BA) were added to the basolateral chamber of the Caco-2 cell monolayers. Transepithelial electrical resistance (TER) was measured at 0, 2, 4, 6, 10, 24, and 48 h after treatment. Data are representative of at least two independent experiments. Values are mean ± S.E. of duplicate (nL-PTC/B) or triplicate (the others) wells. The data were analyzed by two-way ANOVA with Tukey's HSD post hoc test (* $p < 0.05$, *** $p < 0.001$, ns: not significant).

2.4. Toxicities of rL-PTC

The intraperitoneal toxicity of rL-PTCs was assessed by intraperitoneal (i.p.) administration of 200 pg rL-PTCs to mice. L-PTCs absorbed from the intestines or injected into the bloodstream dissociate into BoNT and neurotoxin-associated proteins in the circulation [2,3]. In other words, intraperitoneal injection resulted in the toxicity of BoNT alone in the L-PTC complex. rL-PTC/B-WT, rL-PTC/B-KA, rL-PTC/BA-WT, and rL-PTC/BA-KA all harbored comparable amounts of native BoNT/B (Figure 2) and exhibited similar BoNT toxicity (Figure 5A), indicating that the oral toxicity depends on the intestinal absorption rather than intrinsic BoNT activity.

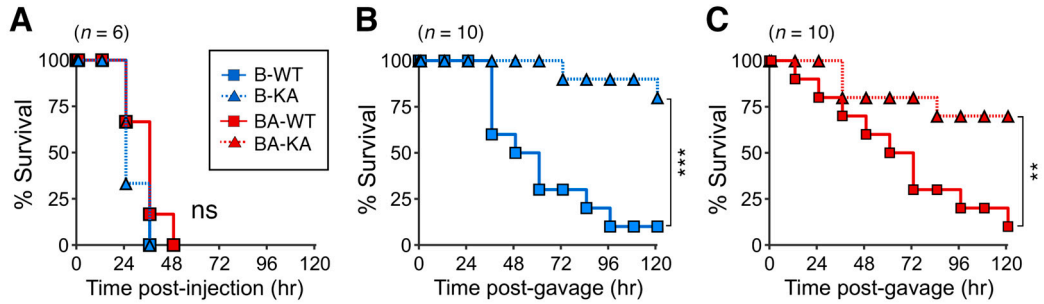


Figure 5. Intraperitoneal and oral toxicities of rL-PTCs in mice. (**A**) Female BALB/c mice were injected i.p. with 100 pg rL-PTCs ($n = 6$/group). (**B**,**C**) Female BALB/c mice were gavaged with 200 ng rL-PTCs/B ($n = 10$/group, (**B**)) and 2 μg r-L-PTCs/BA ($n = 10$/group, (**C**)). ns: not significant, ** $p < 0.01$, *** $p < 0.001$; by log-rank test.

The oral toxicity of rL-PTCs was assessed by intragastrically (i.g.) administering 200 ng of rL-PTCs/B or 2 μg rL-PTCs/BA to mice. rL-PTC/B-WT exhibited at least a 10-fold higher oral toxicity than rL-PTC/BA-WT, indicating that the difference in HA in L-PTC affected oral toxicity (Figure 5B,C) [25]. rL-PTC/B-KA, which lacks barrier-disrupting activity (Figure 4A), exhibited dramatically reduced toxicity (Figure 5B), similar to that of rL-PTC/BA-KA (Figure 5C). These data demonstrate that barrier-disrupting activity is crucial for the oral toxicity of both serotypes, B-Okra and A-62A.

3. Discussion

The large progenitor toxin complex (L-PTC) comprises 14 protein subunits, including BoNT, NTNHA, HA3, HA2, and HA1, in a 1:1:3:3:6 stoichiometry [4–7]. Consistent with a previous study on recombinant L-PTC/A-62A [18], we established an in vitro reconstitu-

tion and purification system for recombinant L-PTCs/B-Okra (rL-PTCs/B) using native BoNT/B-Okra and its recombinant components (Figure 1 and Supplementary Figure S1). We found that the HA3 K607A mutation significantly reduced the oral toxicity of recombinant L-PTC/B-Okra without affecting BoNT activity and carbohydrate-binding. These findings highlight that barrier-disrupting activity is crucial for oral toxicity.

L-PTC/A-62A enters the host through intestinal microfold (M) cells in Peyer's patches [23]. Once in the intestine, the neurotoxin-associated proteins of L-PTC/A-62A disrupts the epithelial barrier around M cells [23]. Additionally, Lee et al. [18] reported that the absence of this barrier-disrupting activity significantly impaired the oral toxicity of recombinant L-PTC/A-62A. The HA of L-PTC/A-62A augmented oral toxicity by compromising the barrier integrity of intestinal M cells. In contrast, hyper-oral-toxic (HOT)-type toxin of serotype B-Okra, unlike non-HOT-type toxin of serotype A-62A, enters the host not only through intestinal M cells but also through the absorptive epithelial cells (enterocytes) of the small intestine [25]. We found that the HA of L-PTC/B disrupts the epithelial barrier of enterocytes in the small intestine [15], and the absence of this activity reduces the oral toxicity of recombinant L-PTC/B-Okra. Together, these findings indicate that HA-mediated barrier disruption facilitates paracellular BoNT uptake through M cells and enterocytes, and that this mechanism contributes to efficient intestinal absorption in HOT- and non-HOT-type toxins.

The intestinal epithelial barrier serves as a boundary between the mucosal immune system and the external environment of the gut lumen [31], yet it also presents a unique opportunity for developing oral delivery systems. For example, M cell-mediated uptake facilitates the entry of antigens [32–36], and transferrin conjugation triggers receptor-mediated transcytosis of cargoes across the intestinal epithelium [37]. The C-terminal fragment of *Clostridium perfringens* enterotoxin (C-CPE) binds to the tight junction (TJ) protein claudin [38,39] and modulates the TJ seal, enabling the paracellular absorption of small molecules [40]. Moreover, HA of botulinum toxin complexes from A-62A and B-Okra can disrupt the E-cadherin–mediated cell–cell adhesion, enabling the paracellular absorption of macromolecules [15,16,23]. These findings suggest that by exploiting multiple intestinal uptake routes—such as transcytosis through M cells and enterocytes in the presence or absence of paracellular transport—engineered toxin-based cargo delivery systems could facilitate efficient mucosal vaccines or therapeutic agents.

4. Materials and Methods

4.1. Plasmid Construction

Genomic DNA was extracted and purified from *C. botulinum* serotype B strain Okra and serotype A strain 62A. NTNHA (aa 1-1197) derived from the serotype B BoNT complex (NTNHA/B)-encoding gene, was cloned into the *Nhe*I-*Sal*I site of the pET28b(+) vector (Merck, Darmstad, Germany) (pET28b-His-NTNHA/B). HA3 (aa 19-626) encoding genes derived from serotype B and A BoNT complexes (HA3/B and HA3/A, respectively) were cloned into the *Kpn*I-*Sal*I site of the pET52b(+) vector (Merck) (pET52b-strep-HA3/B or/A). DNA fragments encoding His-NTNHA/B and strep-HA3s were amplified by PCR and cloned into the *Xba*I-*Sac*I and *Nde*I-*Xho*I sites of pETDuet(+) (Merck) using a GeneArt™ Seamless Cloning and Assembly kit (Thermo Fisher Scientific, Waltham, MA, USA). Site-directed mutagenesis was performed using the PrimeSTAR Max Polymerase (TaKaRa Bio, Shiga, Japan). The inserted regions of these plasmids and the presence of mutations were confirmed using DNA sequencing.

4.2. Protein Expression and Purification

To obtain the recombinant HA3-NTNHA (rHA3-NTNHA) complexes, *Escherichia coli* Rosetta2 (DE3) cells (Merck) transformed with the co-expression plasmids were grown in Terrific Broth (TB) media. Protein expression was induced using the Overnight Express™ Autoinduction System 1 (Merck) at 18 °C for 48 h. The cells were then harvested and lysed in a lysis buffer (50 mM Tris-HCl, pH 7.4, and 300 mM NaCl) by sonication. The His-tagged proteins were bound to HisTrap HP (Cytiva, Marlborough, MA, USA) and eluted with His elution buffer (50 mM Tris-HCl pH 7.4, 300 mM NaCl, 300 mM imidazole). To purify the HA3-NTNHA complex, the eluates were loaded onto StrepTrap HP (Cytiva) equilibrated with PBS (pH 7.4), and the bound proteins were eluted with 3 mM D-desthiobiotin.

Recombinant FLAG-tagged HA1 serotypes B and A (rHA1/B-FLAG and rHA1/A-FLAG, respectively) and recombinant FLAG-tagged HA2 serotypes B and A (FLAG-rHA2/B and FLAG-rHA2/A, respectively) were prepared as previously described [13]. Native BoNT serotype B-Okra (nBoNT/B) was prepared as described previously [41].

All proteins were dialyzed against PBS (pH 7.4 or 6.0) and stored at −80 °C until needed. Protein concentrations of the samples were determined using a Pierce BCA assay (Thermo Fisher Scientific).

4.3. In Vitro Reconstitution and Purification

To reconstitute recombinant HA complexes (rHA: HA1 + HA2 + HA3), recombinant HA1, HA2, and HA3 proteins were mixed at a molar ratio of 4:4:1 in PBS (pH 7.4). To reconstitute recombinant NAP complexes (rNAP: NTNHA + HA), recombinant HA1, HA2, and HA3-NTNHA were mixed at a molar ratio of 12:12:1 in PBS (pH 7.4). The mixtures were then incubated at 37 °C for 3 h. The complexes were purified using StrepTrap HP and dialyzed against phosphate-buffered saline PBS (pH 6.0).

To reconstitute recombinant L-PTC (rL-PTC), nBoNT/B and rNAP proteins were mixed at a molar ratio of 3:1 in PBS (pH 6.0) and incubated at 37 °C for 3 h. The rL-PTCs were bound to a-Lactose gels (EY laboratories, San Mateo, CA, USA) equilibrated with PBS (pH 6.0) and then eluted with 0.2 M lactose. Purified proteins were dialyzed against PBS (pH 6.0). The protein concentrations of the samples were determined using a Pierce BCA assay.

4.4. Size Exclusion Chromatography

10 μg of each protein (rHA1/B, rHA/2, rHA3, rNTNHA/B, rNTNHA/B-rHA3/B, rHA/B, rNAP/B, native BoNT/B, rL-PTC/B-WT, and native L-PTC/B) was loaded onto a Superdex 200 Increase 10/300 GL column (Cytiva) equilibrated with PBS (pH 6.0) using ÄKTA pure (Cytiva). Elution was performed with the same buffer at a flow rate of 0.75 mL/min and monitored by the absorbance at 280 nm.

4.5. Western Blotting

Equimolar amounts of protein (native L-PTC/B, rL-PTC/B-WT, rL-PTC/B-KA, rL-PTC/BA-WT, and rL-PTC/BA-KA) were separated by 15% SDS-PAGE and transferred onto Immobilon-P™ PVDF membranes (Merck). After blocking with 5% skim milk, the membranes were incubated with antibodies against BoNT/B (rabbit, anti-serum [15]), His tag (mouse monoclonal Ab, clone OGHis, MBL, Tokyo, Japan), Strep-tag II tag (mouse monoclonal Ab, Cat. 71590-3, Merck), and FLAG tag (mouse monoclonal Ab, clone M2, Merck), followed by appropriate HRP-conjugated secondary antibodies (Jackson ImmunoResearch, West Grove, PA, USA). Subsequently, the membranes were developed using ECL Select (Cytiva) and visualized with an ImageQuant™ LAS 4000 mini (Cytiva).

4.6. Mucin ELISA

96-well ELISA plates (IWAKI, Tokyo, Japan) were coated with 100 ng/mL porcine gastric mucin (PGM; M1778, Sigma, Darmstad, Germany) and bovine submaxillary mucin (BSM; M3895, Sigma) at 37 °C for 1 hr. After blocking with 1% BSA/PBS-T (pH 6.0), the plates were incubated with 10 nM L-PTCs or HAs at 37 °C for 1 hr. After washing with PBS-T (pH 6.0), the plates were probed with antibodies against BoNT/B or FLAG tags, followed by incubation with the appropriate HRP-conjugated secondary antibodies. Subsequently, the plates were developed using ABTS (Merck), and the absorbance at 405 nm was measured.

4.7. Transepithelial Electrical Resistance (TER) Assay

TER was measured using a Millicell-ERS (Merck), as described previously [15]. Briefly, Caco-2 cell monolayers were established on Transwell^{TM} filters (Corning, Glendale, AZ, USA) and 10 nM L-PTCs or HAs were added to the basolateral chambers. TER was measured at different time points up to 48 h post-addition.

4.8. Mouse Bioassay

Female BALB/c mice aged 7–8 wk were purchased from Japan SLC, (Shizuoka, Japan). The mice were fasted for 4 h before the challenge. For intraperitoneal (i.p.) administration, the mice were injected i.p. with 100 pg of rL-PTCs in 300 µL of bioassay buffer (0.1% gelatin, 10 mM NaPi, pH 6.0). For intragastric (i.g.) administration, the mice were gavaged i.g., with 200 ng of rL-PTCs/B or 2 µg of rL-PTCs/BA in 300 µL of bioassay buffer. The mice were re-fed 1 h after the challenge, and the survival rate was assessed every 12 h over the subsequent five days. The toxins were administered in a single-blind manner, and intoxication was scored by two investigators.

4.9. Statistical Analysis

Statistical testing was performed using RStudio (R version 4.1.2) and Prism 10 (GraphPad Software, Boston, MA, USA). Statistical significance was evaluated using one- or two-way ANOVA with Tukey's HSD post hoc test. Differences with $p < 0.05$ were considered statistically significant.

Supplementary Materials: The following supporting information can be downloaded at https://www.mdpi.com/article/10.3390/toxins17090443/s1, Figure S1: Schematic model of protein preparation.

Author Contributions: Conceptualization, S.A.; investigation, C.M., S.A. and T.M.; data analysis, M.Z.; data curation, C.M. and S.A.; writing—original draft preparation, S.A.; writing—review and editing, S.A. and Y.F.; supervision, Y.F. All authors have read and agreed to the published version of the manuscript.

Funding: This research was funded by the Japan Society for the Promotion of Science (JSPS) KAKENHI, Grant Numbers 19K21257, 20K16240, and 23K14517 to S. A.

Institutional Review Board Statement: All animal experiments were approved by the Animal Experiment Committee of Kanazawa University (AP-163708; approval on 21 April 2017) and performed in accordance with the guidelines and regulations of Kanazawa University. All bacterial experiments using *Clostridium botulinum* were conducted in the Fujinaga Lab, approved by the biosafety committee of Kanazawa University and the Minister of Health, Labour and Welfare of Japan.

Informed Consent Statement: Not applicable.

Data Availability Statement: The original contributions presented in this study are included in the article/Supplementary Material. Further inquiries can be directed to the corresponding author(s).

Acknowledgments: We thank Mayu Kitamura and Sachiyo Akagi for their technical assistance, and the members of the Fujinaga Lab for helpful discussion.

Conflicts of Interest: The authors declare no conflicts of interest.

Abbreviations

BoNT, botulinum neurotoxin; BSM, bovine submaxillary mucin; HA, hemagglutinin; HOT type, high-oral-toxic type; i.p., intraperitoneal; i.g., intragastric; KA, K607A; L-PTC, large progenitor toxin complex; M-PTC, medium progenitor toxin complex; M cell, microfold cell; NAP, neurotoxin-associated protein; nBoNT, native BoNT; nL-PTC, native L-PTC; NTNHA, non-toxic non-hemagglutinin; PGM, porcine gastric mucin;rL-PTC, recombinant L-PTC; rNAP, recombinant NAP; rNTNHA, recombinant NTNHA; rHA, recombinant HA; TER, transepithelial electrical resistance; WT, wild-type.

References

1. Schiavo, G.; Matteoli, M.; Montecucco, C. Neurotoxins Affecting Neuroexocytosis. *Physiol. Rev.* **2000**, *80*, 717–766. [CrossRef]
2. Sakaguchi, G. *Clostridium Botulinum* Toxins. *Pharmacol. Ther.* **1982**, *19*, 165–194. [CrossRef] [PubMed]
3. Sugii, S.; Ohishi, I.; Sakaguchi, G. Correlation between Oral Toxicity and in Vitro Stability of *Clostridium botulinum* Type A and B Toxins of Different Molecular Sizes. *Infect. Immun.* **1977**, *16*, 910–914. [CrossRef]
4. Amatsu, S.; Sugawara, Y.; Matsumura, T.; Kitadokoro, K.; Fujinaga, Y. Crystal Structure of *Clostridium botulinum* Whole Hemagglutinin Reveals a Huge Triskelion-Shaped Molecular Complex. *J. Biol. Chem.* **2013**, *288*, 35617–35625. [CrossRef] [PubMed]
5. Lee, K.; Gu, S.; Jin, L.; Le, T.T.N.; Cheng, L.W.; Strotmeier, J.; Kruel, A.M.; Yao, G.; Perry, K.; Rummel, A.; et al. Structure of a Bimodular Botulinum Neurotoxin Complex Provides Insights into Its Oral Toxicity. *PLoS Pathog.* **2013**, *9*, e1003690. [CrossRef]
6. Benefield, D.A.; Dessain, S.K.; Shine, N.; Ohi, M.D.; Lacy, D.B. Molecular Assembly of Botulinum Neurotoxin Progenitor Complexes. *Proc. Natl. Acad. Sci. USA* **2013**, *110*, 5630–5635. [CrossRef] [PubMed]
7. Hasegawa, K.; Watanabe, T.; Suzuki, T.; Yamano, A.; Oikawa, T.; Sato, Y.; Kouguchi, H.; Yoneyama, T.; Niwa, K.; Ikeda, T.; et al. A Novel Subunit Structure of *Clostridium Botulinum* Serotype D Toxin Complex with Three Extended Arms. *J. Biol. Chem.* **2007**, *282*, 24777–24783. [CrossRef]
8. Ohishi, I. Oral Toxicities of *Clostridium botulinum* Type A and B Toxins from Different Strains. *Infect. Immun.* **1984**, *43*, 487–490. [CrossRef]
9. Fujinaga, Y.; Inoue, K.; Watanabe, S.; Yokota, K.; Hirai, Y.; Nagamachi, E.; Oguma, K. The Haemagglutinin of *Clostridium botulinum* Type C Progenitor Toxin Plays an Essential Role in Binding of Toxin to the Epithelial Cells of Guinea Pig Small Intestine, Leading to the Efficient Absorption of the Toxin. *Microbiology* **1997**, *143*, 3841–3847. [CrossRef]
10. Inoue, K.; Sobhany, M.; Transue, T.R.; Oguma, K.; Pedersen, L.C.; Negishi, M. Structural Analysis by X-Ray Crystallography and Calorimetry of a Haemagglutinin Component (HA1) of the Progenitor Toxin from *Clostridium botulinum*. *Microbiology* **2003**, *149*, 3361–3370. [CrossRef]
11. Lee, K.; Lam, K.H.; Kruel, A.M.; Perry, K.; Rummel, A.; Jin, R. High-Resolution Crystal Structure of HA33 of Botulinum Neurotoxin Type B Progenitor Toxin Complex. *Biochem. Biophys. Res. Commun.* **2014**, *446*, 568–573. [CrossRef] [PubMed]
12. Tulin, E.K.C.; Nakazawa, C.; Nakamura, T.; Saito, S.; Phzono, N.; Hiemori, K.; Nakakita, S.I.; Tateno, H.; Tonozuka, T.; Nishikawa, A. Glycan Detecting Tools Developed from the *Clostridium botulinum* Whole Hemagglutinin Complex. *Sci. Rep.* **2021**, *11*, 21973. [CrossRef]
13. Amatsu, S.; Matsumura, T.; Yutani, M.; Fujinaga, Y. Multivalency Effects of Hemagglutinin Component of Type B Botulinum Neurotoxin Complex on Epithelial Barrier Disruption: Multivalency Effect of HA. *Microbiol. Immunol.* **2018**, *62*, 80–89. [CrossRef]
14. Amatsu, S.; Fujinaga, Y. Botulinum Hemagglutinin: Critical Protein for Adhesion and Absorption of Neurotoxin Complex in Host Intestine. *Methods Mol. Biol.* **2020**, *2132*, 183–190. [CrossRef] [PubMed]
15. Matsumura, T.; Jin, Y.; Kabumoto, Y.; Takegahara, Y.; Oguma, K.; Lencer, W.I.; Fujinaga, Y. The HA Proteins of Botulinum Toxin Disrupt Intestinal Epithelial Intercellular Junctions to Increase Toxin Absorption. *Cell. Microbiol.* **2008**, *10*, 355–364. [CrossRef]
16. Sugawara, Y.; Matsumura, T.; Takegahara, Y.; Jin, Y.; Tsukasaki, Y.; Takeichi, M.; Fujinaga, Y. Botulinum Hemagglutinin Disrupts the Intercellular Epithelial Barrier by Directly Binding E-Cadherin. *J. Cell Biol.* **2010**, *189*, 691–700. [CrossRef]

17. Sugawara, Y.; Yutani, M.; Amatsu, S.; Matsumura, T.; Fujinaga, Y. Functional Dissection of the *Clostridium botulinum* Type B Hemagglutinin Complex: Identification of the Carbohydrate and E-Cadherin Binding Sites. *PLoS ONE* **2014**, *9*, e111170. [CrossRef]
18. Lee, K.; Zhong, X.; Gu, S.; Kruel, A.M.; Dorner, M.B.; Perry, K.; Rummel, A.; Dong, M.; Jin, R. Molecular Basis for Disruption of E-Cadherin Adhesion by Botulinum Neurotoxin A Complex. *Science* **2014**, *344*, 1405–1410. [CrossRef]
19. Amatsu, S.; Matsumura, T.; Zuka, M.; Fujinaga, Y. Molecular Engineering of a Minimal E-Cadherin Inhibitor Protein Derived from *Clostridium botulinum* Hemagglutinin. *J. Biol. Chem.* **2023**, *299*. [CrossRef]
20. Fujinaga, Y.; Inoue, K.; Nomura, T.; Sasaki, J.; Marvaud, J.C.; Popoff, M.R.; Kozaki, S.; Oguma, K. Identification and Characterization of Functional Subunits of *Clostridium botulinum* Type A Progenitor Toxin Involved in Binding to Intestinal Microvilli and Erythrocytes. *FEBS Lett.* **2000**, *467*, 179–183. [CrossRef] [PubMed]
21. Arimitsu, H.; Sakaguchi, Y.; Lee, J.C.; Ochi, S.; Tsukamoto, K.; Yamamoto, Y.; Ma, S.; Tsuji, T.; Oguma, K. Molecular Properties of Each Subcomponent in *Clostridium botulinum* Type B Haemagglutinin Complex. *Microb. Pathog.* **2008**, *45*, 142–149. [CrossRef] [PubMed]
22. Yao, G.; Lee, K.; Gu, S.; Lam, K.H.; Jin, R. Botulinum Neurotoxin A Complex Recognizes Host Carbohydrates through Its Hemagglutinin Component. *Toxins* **2014**, *6*, 624–635. [CrossRef]
23. Matsumura, T.; Sugawara, Y.; Yutani, M.; Amatsu, S.; Yagita, H.; Kohda, T.; Fukuoka, S.I.; Nakamura, Y.; Fukuda, S.; Hase, K.; et al. Botulinum Toxin A Complex Exploits Intestinal M Cells to Enter the Host and Exert Neurotoxicity. *Nat. Commun.* **2015**, *6*, 6255. [CrossRef]
24. Lam, T.I.; Stanker, L.H.; Lee, K.; Jin, R.; Cheng, L.W. Translocation of Botulinum Neurotoxin Serotype A and Associated Proteins across the Intestinal Epithelia. *Cell. Microbiol.* **2015**, *17*, 1133–1143. [CrossRef]
25. Amatsu, S.; Matsumura, T.; Morimoto, C.; Keisham, S.; Goto, Y.; Kohda, T.; Hirabayashi, J.; Kitadokoro, K.; Katayama, T.; Kiyono, H.; et al. Gut Mucin Fucosylation Dictates the Entry of Botulinum Toxin Complexes. *bioRxiv* **2025**. [CrossRef]
26. Hill, K.K.; Smith, T.J. Genetic Diversity Within *Clostridium botulinum* Serotypes, Botulinum Neurotoxin Gene Clusters and Toxin Subtypes. *Curr. Top. Microbiol. Immunol.* **2013**, *364*, 1–20. [CrossRef]
27. Gao, L.; Nowakowska, M.B.; Selby, K.; Przykopanski, A.; Chen, B.; Krüger, M.; Douillard, F.P.; Lam, K.H.; Chen, P.; Huang, T.; et al. Botulinum Neurotoxins Exploit Host Digestive Proteases to Boost Their Oral Toxicity via Activating OrfXs/P47. *Nat. Struct. Mol. Biol.* **2025**, *32*, 864–875. [CrossRef]
28. Arnon, S.S.; Schechter, R.; Inglesby, T.V.; Henderson, D.A.; Bartlett, J.G.; Ascher, M.S.; Eitzen, E.; Fine, A.D.; Hauer, J.; Layton, M.; et al. Botulinum Toxin as a Biological Weapon: Medical and Public Health Management. *JAMA* **2001**, *285*, 1059–1070. [CrossRef]
29. Ohno, H.; Hase, K. Glycoprotein 2 (GP2): Grabbing the FimH bacteria into M cells for mucosal immunity. *Gut Microbes* **2010**, *1*, 407–410. [CrossRef] [PubMed]
30. Van Der Flier, L.G.; Clevers, H. Stem Cells, Self-Renewal, and Differentiation in the Intestinal Epithelium. *Annu. Rev. Physiol.* **2009**, *71*, 241–260. [CrossRef] [PubMed]
31. McGuckin, M.A.; Lindén, S.K.; Sutton, P.; Florin, T.H. Mucin Dynamics and Enteric Pathogens. *Nat. Rev. Microbiol.* **2011**, *9*, 265–278. [CrossRef]
32. Wu, Y.; Wang, X.; Csencsits, K.L.; Haddad, A.; Walters, N.; Pascual, D.W. M Cell-Targeted DNA Vaccination. *Proc. Natl. Acad. Sci. USA* **2001**, *98*, 9318–9323. [CrossRef]
33. Shima, H.; Watanabe, T.; Fukuda, S.; Fukuoka, S.I.; Ohara, O.; Ohno, H. A Novel Mucosal Vaccine Targeting Peyer's Patch M Cells Induces Protective Antigen-Specific IgA Responses. *Int. Immun.* **2014**, *26*, 619–625. [CrossRef]
34. Nochi, T.; Takagi, H.; Yuki, Y.; Yang, L.; Masumura, T.; Mejima, M.; Nakanishi, U.; Matsumura, A.; Uozumi, A.; Hiroi, T.; et al. Rice-Based Mucosal Vaccine as a Global Strategy for Cold-Chain- and Needle-Free Vaccination. *Proc. Natl. Acad. Sci. USA* **2007**, *104*, 10986–10991. [CrossRef] [PubMed]
35. Yamamoto, M.; Pascual, D.W.; Kiyono, H. M Cell-Targeted Mucosal Vaccine Strategies. *Curr. Top. Microbiol. Immunol.* **2012**, *354*, 39–52. [CrossRef]
36. Nochi, T.; Yuki, Y.; Matsumura, A.; Mejima, M.; Terahara, K.; Kim, D.Y.; Fukuyama, S.; Iwatsuki-Horimoto, K.; Kawaoka, Y.; Kohda, T.; et al. A Novel M Cell–Specific Carbohydrate-Targeted Mucosal Vaccine Effectively Induces Antigen-Specific Immune Responses. *J. Exp. Med.* **2007**, *204*, 2789–2796. [CrossRef] [PubMed]
37. Zou, J.J.; Wei, G.; Xiong, C.; Yu, Y.; Li, S.; Hu, L.; Ma, S.; Tian, J. Efficient Oral Insulin Delivery Enabled by Transferrin-Coated Acid-Resistant Metal-Organic Framework Nanoparticles. *Sci. Adv.* **2022**, *8*, eabm4677. [CrossRef]
38. Suzuki, H.; Tani, K.; Fujiyoshi, Y. Crystal Structures of Claudins: Insights into Their Intermolecular Interactions. *Ann. N. Y. Acad. Sci.* **2017**, *1397*, 25–34. [CrossRef]
39. Katahira, J.; Sugiyama, H.; Inoue, N.; Horiguchi, Y.; Matsuda, M.; Sugimoto, N. *Clostridium perfringens* Enterotoxin Utilizes Two Structurally Related Membrane Proteins as Functional Receptors in Vivo. *J. Biol. Chem.* **1997**, *272*, 26652–26658. [CrossRef] [PubMed]

40. Kondoh, M.; Masuyama, A.; Takahashi, A.; Asano, N.; Mizuguchi, H.; Koizumi, N.; Fujii, M.; Hayakawa, T.; Horiguchi, Y.; Watanbe, Y. A Novel Strategy for the Enhancement of Drug Absorption Using a Claudin Modulator. *Mol. Pharmacol.* **2005**, *67*, 749–756. [CrossRef] [PubMed]
41. Matsumura, T.; Amatsu, S.; Misaki, R.; Yutani, M.; Du, A.; Kohda, T.; Fujiyama, K.; Ikuta, K.; Fujinaga, Y. Fully Human Monoclonal Antibodies Effectively Neutralizing Botulinum Neurotoxin Serotype, B. *Toxins* **2020**, *12*, 302. [CrossRef] [PubMed]

Disclaimer/Publisher's Note: The statements, opinions and data contained in all publications are solely those of the individual author(s) and contributor(s) and not of MDPI and/or the editor(s). MDPI and/or the editor(s) disclaim responsibility for any injury to people or property resulting from any ideas, methods, instructions or products referred to in the content.